Applied Rheology

To appear as: Appl. Rheol. 20 (2010) 62402
DOI: 10.3933/ApplRheol-20-62402

DETERMINATION OF THE RHEOLOGICAL PARAMETERS OF SELF-COMPACTING CONCRETE MATRIX USING SLUMP FLOW TEST

Marina K.-A. Neophytou*, Stella Pourgouri, Antonios D. Kanellopoulos, Michael F. Petrou, Ioannis Ioannou, Georgios Georgiou[1] and Andreas Alexandrou[2]

Department of Civil and Environmental Engineering, University of Cyprus, 1678 Nicosia, Cyprus
[1] Department of Mathematics and Statistics, University of Cyprus, 1678 Nicosia, Cyprus
[2] Department of Mechanical and Manufacturing Engineering, University of Cyprus, 1678 Nicosia, Cyprus

email: neophytou@ucy.ac.cy
Fax: x357.2289.2295

Received: 9.3.2010, Final version: 7.7.2010

Abstract:
The classification of a concrete mixture as self-compacting (SCC) is performed by a series of empirical characterization tests that have been designed to assess not only the flowability of the mixture but also its segregation resistance and filling ability. The objective of the present work is to correlate the rheological parameters of SCC matrix, yield stress and plastic viscosity, to slump flow measurements. The focus of the slump flow test investigation was centered on the fully yielded flow regime and an empirical model relating the yield stress to material and flow parameters is proposed. Our experimental data revealed that the time for a spread of 500 mm which is used in engineering practice as reference for measurement parameters, is an arbitrary choice. Our findings indicate that the non-dimensional final spread is linearly related to the non-dimensional yield-stress. Finally,there are strong indications that the non-dimensional viscosity of the mixture is associated with the non-dimensional final spread as well as the stopping time of the slump flow; this experimental data set suggests an exponential decay of the final spread and stopping time with viscosity.

Key words: self compacting concrete, rheology, slump flow, yield stress, dimensional analysis

1 INTRODUCTION

The rheology of fresh concrete has been the subject of many studies in the past few decades. Fresh concrete can be viewed as a concentrated suspension of solid particles (aggregates) in a viscous medium, i.e. cement paste. The latter is also a concentrated suspension of cement grains in water. As many other suspensions, fresh concrete is a thixotropic material exhibiting yield stress [1]. A complete review of the constitutive equations used for cement-based materials is provided by Yahia and Khayat [2]. The most popular constitutive equation used to describe such behaviour is the Bingham model:

$$\left.\begin{array}{ll} \tau=\tau_o+\mu\dot{\gamma} & \tau\geq\tau_o \\ \dot{\gamma}=0 & \tau\leq\tau_o \end{array}\right\} \qquad (1)$$

where τ is the shear stress (Pa), $\dot{\gamma}$ is the shear rate (1/s), τ_0 is the yield stress (Pa), and μ is the plastic viscosity (Pa·s). The yield stress is the critical shear stress required to initiate deformation (flow). The plastic viscosity describes the resistance to flow once the yield stress is exceeded. If the yield stress is zero, the Bingham model is reduced to the Newtonian model:

$$\tau=\mu\dot{\gamma} \qquad (2)$$

where μ represents the constant viscosity. The two material parameters τ_0 and μ in the Bingham plastic model are in general time-dependent. Time influences these properties, in addition to thixotropic effects due to hydration [3 - 5]. In general, both yield stress and plastic viscosity increase with time, as the concrete hardens [6, 7]. These two rheological properties are necessary in order to quantitatively describe the flow of fresh concrete. Thus, they are very critical for the concrete industry because they determine concrete placement and workability. However, in most studies only the steady-state values of the rheological parameters are considered, which implies that thixotropy is not taken into account. This in turn means that loss of workability is not modelled [4]. In general, SCCs are designed with low yield stresses ranging from zero to 60 Pa while the plastic viscosity varies from 20 to 100 Pa·s [8]. Experiments indicate that SCCs exhibit shear thickening behaviour: the apparent viscosity increases with shear rate. Thus, shear thickening becomes important in operations occurring at high shear rates, like mixing and pumping [4, 9, 10]. This behaviour can be described by a generalization of the Bingham model, known as the Herschel-Bulkley model:

$$\left.\begin{array}{ll} \tau = \tau_o + K\dot{\gamma}^n & \tau \geq \tau_o \\ \dot{\gamma} = 0 & \tau \leq \tau_o \end{array}\right\} \quad (3)$$

where K is the consistency index and n is the (dimensionless) power-law exponent or flow index. For $n = 1$ the Bingham model is recovered. The Herschel-Bulkley model has been used to describe the rheology of fresh concrete [11, 12]. Shear thickening corresponds to $n > 1$, whereas $n < 1$ corresponds to shear thinning. Ferraris [11] reported a mean value of 1.53 for n in the case of concrete without a superplasticizer and of 1.36 for other concretes. As already mentioned, the determination of the rheological parameters is of crucial importance, since these parameters affect the workability and the placement of fresh concrete. The former includes high fluidity, deformability, good filling ability, and moderate resistance to segregation [13], while the latter includes transportation, pumping, casting and vibration [14]. Moreover, the quality of hardened concrete is also affected by the flow behaviour of fresh concrete.

In principle, optimal design of SCC should allow for the easy flow movement of the fresh material around flow obstacles under its own weight [15]. However, at the same time, improving SCC flowability should not jeopardise essential physical and mechanical properties and it should not cause any segregation. Despite being satisfactory in standard operational practice, empirical tests widely used so far to assess an "apparent" rheology and thereby SCC flowability still lack transparency in physical meaningfulness, largely due to the complexity of the concrete mixtures [16, 17]. The measurement of rheological parameters has been central to the design of SCC, as they relate to the flowability and segregation resistance of the fluid. While such parameters have been most commonly measured so far using standard falling-ball viscometers for Newtonian fluids and specially designed rheometers for Bingham and other fluids [18 - 20], for SCC there have been a number of empirical tests (slump flow test, V-Funnel, L-Box test, U-Box test, J-Ring, wet sieve segregation and surface settlement tests) proposed and established in practice [13]. These tests are simple enough to implement on site on one hand, and on the other, to attempt to capture the rheological complexity of fluids such as SCC.

In a recent study [21] there has been an effort to relate measurement parameters of empirical tests (such as the slump flow test) to the rheological parameters of SCC. The slump test, in its original form, is the most widely used test method to characterize the workability of fresh concrete. The set-up of the method consists of a frustum of a metallic cone with base radius (r_0) 0.1 m, which is filled with concrete. The cone is lifted vertically allowing the concrete to move and the reduction in height (slump) of the fresh concrete is measured. Slump is influenced by both yield stress and viscosity; however, for most cases the effect of viscosity is considered negligible. As simple as the slump test may be, it is a complex time-dependent free-surface flow which is difficult to simulate [22]. The vast majority of existing models regarding the slump test, have been developed based on the idea of connecting the slump with the yield stress of the material. Pashias et al. [23] adapted the dimensionless slump model for cylindrical geometries developing a numerical model that correlated the yield stress of concrete to its slump. The measurement is not affected by the type of flocculated material being tested. The model was found to be in agreement with experimental measurements. Their study showed that the final slump of the material is largely independent of the lifting rate and surface on which the slump test is performed. Saak et al. [24] also developed a dimensionless model relating slump to yield stress. The model was further improved and generalised as a function of cone geometry. The results of Saak et al. [24] showed that the simulation fits the experimental data for cylindrical slump over a wide range of yield stress values for a variety of materials. As in the case of the model developed by Pashias et al. [23], their model also deals with materials that exhibit slump rather than spread.

The slump flow test, which is a modification of the traditional slump test, in which the spread of the material is measured instead of the height reduction, is the simplest and most commonly used test for evaluating SCC [23]. The test involves the use of a conventional slump cone. The cone is placed on a rigid, non-absorbent plate on a firm, level surface and is filled with concrete without tamping. The slump cone is lifted and the horizontal spread of the concrete is measured. Slump flow or spreading is the average diameter of three measurements of the spread after stabilization. The time required for the material to spread to a diameter of 500 mm is also measured providing another measure of flowability. This time, denoted by T_{500}, varies from 2-7 seconds in the case of fresh SCC. However, the test is operator-dependent. To account for this factor in this study the same operator was used for all cone lifting tests discussed in later sections. In this way the uncertainty raised between different operators is eliminated. According to Koehler and Fowler [26] the results of the slump flow test are influenced by the changing and unknown stresses acting within the specimen during the tests.

Esping [27] presented experimental results for self-compacting concrete showing that the slump flow spread is not a unique function of yield stress, but rather a more complex function of both yield stress and plastic viscosity. On the other hand, the same author noted that the spread is more closely related to the yield stress than to the viscosity, especially at high viscosities, whereas the T_{500} was linked equally with both yield stress and viscosity. Recently, Feys et al. [4] used slump flow test results in order to investigate two possible theories for shear thickening of SCC while Kou and Poon [5] presented some slump flow data of SCC mixtures incorporating recycled glass aggregate, which showed that the flowability (i.e. slump flow) decreases linearly with time due to the hydration of cement.

Roussel and Coussot [28] focused on modifying the fundamental concepts of the models for the slump test described above in order to account for the spread of the material. They used a cone with cylindrical coordinates and made a distinction between the possible flow regimes. Consequently, two different flow regimes were identified (slump and flow), and equations were derived that connect the yield stress of the material to its slump and spreading distance. Numerical simulations showed very good correlation with the experimental results. However, the model developed did not account for thixotropic effects, which may significantly alter the data [29-30]. Similar observations concerning the importance of thixotropic effects on fresh cement pastes are also reported by Jarni et al. [31].

The complex synthesis of the SCC mixture adds a further complication in any attempt to model the flow of the material. Even though some work has been done towards correlating the yield stress of SCC to the mixture proportions [32, 33], there is still room for improvement; the proposed models incorporate a certain number of assumptions and empirical factors which strictly relate to specific mixtures examined. Therefore, it is not certain whether such analytical approaches can be easily generalised. Recent experimental work [34] links specifically the slump flow spread to the reference flow time (T_{500}), as well as to the yield stress and the viscosity of the mixture. The results suggest that the slump flow spread and T_{500} time are not unique functions of yield stress and viscosity respectively. Moreover, the spread seems to be more closely connected to the yield stress than the viscosity, especially at high viscosities, while T_{500} time is better linked with yield stress and viscosity [27]. Consequently, the authors conclude that T_{500} can only be used to estimate the viscosity of a mixture with constant yield stress, while slump flow can be used to estimate the yield stress with constant viscosity.

Further recent research studies have shown that empirical equations can be derived providing a link between the Bingham parameters of cement-based composites (cement pastes, conventional concrete, and SCC) and the time required to achieve final spread [32 - 35]; at the same time, some other research studies have shown that there is no correlation between Bingham parameters and the slump flow test, highlighting the requirement for alternate test methods [36, 37]. Another study [38] revealed that empirical equations can be derived connecting the viscosity of SCC to the time required to reach its final spread. In this study, it was observed that there is a connection between viscosity and the time needed for resting at maximum spread (the higher the viscosity, the higher the required time), but hardly any reliable correlation could be found [38]. This was due to the fact that adjacent values of viscosity resulted in quite different values of spread time.

It is therefore evident from the above literature review that in the past two decades there have been many attempts to correlate the rheological parameters of SCC to empirical tests. In the case of the slump test, the connection between the Herschel-Bulkley yield stress and the slump has been proved both theoretically and experimentally [11, 22 - 24, 39, 40]. Roussel et al. [41] also proposed an analytical correlation between spread and yield stress of cement pastes. Nguyen et al. [42] proposed a theoretical analysis of the L-box test for homogeneous flow, correlated the theoretical shape of the sample to experimental results on limestone powder suspensions, and suggested practical applications of their analysis to the case of SCC.

The factors affecting the flow of fresh concrete were evaluated by Kurokawa et al. [43] who used the so-called viscoplastic finite element method to simulate it as a Bingham plastic fluid. Thrane et al. [44] also employed the Bingham plastic model and used a commercial code to simulate the flow of SCC in both L-box and slump tests. However, the material constants in this case were measured in a BML rheometer. Roussel and Coussot [28] and Roussel [1] used another code to perform three-dimensional simulations of the flow of concrete in different slump tests. Their simulations confirmed that slump depends only on yield stress and density. Dufour and Pijaudier-Cabot [45] applied a finite element method with Lagrange integration points (FEMLIP) to simulate the flow of ordinary, self-compacting and high-performance concrete and calibrated the two material parameters of the Bingham model from experimental results from a simple slump test with flow time measurement. Koehler and Fowler [26] measured the rheological properties of SCC by means of a new portable rheometer and then related these properties to the slump flow and T_{500} results. Their results indicated that slump flow decreas-

To appear as: Appl. Rheol. 20 (2010) 62402
DOI: 10.3933/ApplRheol-20-62402

es linearly with yield stress and that T_{500} increases linearly with the plastic viscosity.

This paper focuses on the slump flow test for fresh SCC matrix. It addresses the connection of the slump flow test measurements to the SCC matrix rheological parameters making use of dimensional analysis and a unique experimental procedure. For comparison purposes and in order to validate the model, experiments have also been carried out on glycerine at different temperatures (Newtonian fluids) and on Carbopol mixtures at different concentrations (Bingham plastic fluids). In Section 2, the conceptual basis of the model as well as the dimensional analysis are discussed. In Section 3 the methodology for the slump flow experiments is described. In Section 4, the experimental results are presented and the dependence of the final spread and the stopping time on the material parameters, i.e. the yield stress and the plastic viscosity, is demonstrated. The conclusions of this work are summarized in Section 5.

2 CONCEPTUAL BASIS AND DIMENSIONAL ANALYSIS

During the process of a slump flow test, the resulting flow of the fresh concrete mixture is determined by an interplay between the pressure distribution in the conical column with an initial height H, and the resistance to deformation due to the yield stress τ_0 and to a lesser extent the viscous forces due to the viscosity of the fluid μ. Key characteristic stresses are then τ_0 and ρgH, where ρ is the density of the mixture and g is the gravitational acceleration. At the limit, when the original height $H \approx \tau_0/\rho g$, i.e. when the maximum stress in the sample is equal to (or less than) the yield stress, the sample does not deform and hence there is no flow. Flow occurs when H is greater than $\tau_0/\rho g$. Conventionally then if we define $X = \rho gH/\tau_0$, yielding or flow is a function of X. Therefore, when $X \leq 1$ there is no flow and when $X > 1$ the sample deforms. Once flow is initiated the bulk of the material collapses while, due to symmetry, it simultaneously spreads radially. The rate of spreading of course is related to the rate of "collapse" through mass conservation. Characteristic collapsing velocity due this gravity driven flow is $U = \sqrt{(gh)}$. Characteristic scales are both the initial height H and the volume of the column, V , because they collectively define X.

Figure 1 is a schematic of the expected flow characteristics based on the physics of the problem. The flow domain is characterized by three distinct regions: (a) stagnant flow, (b) fully yielded shear flow and (c) unyielded plug flow. The stagnant flow is expected to form around the axis of symmetry close to the radial axis due to the symmetry conditions of the flow field. The plug flow is unyielded material that moves as a solid body and the fully-yielded material are regions of high shear where the local stresses exceed the yield stress. As shown in Figure 1 due to the free surface boundary conditions the unyielded material is expected to "ride" on top of the shear region. The above is only a general schematic. The exact flow map and the details of the transition from one region to another can be determined only with detailed simulations.

In a dimensional analysis, a reference flow velocity U and a final spread S can be considered as characteristic parameters which are in turn determined by the viscosity of the mixture, the density, ρ, the collapsing velocity due to gravity as defined by the height, H, of the sample and the gravitational acceleration, g. These can be expressed in dimensional form as:

$$\frac{U}{\sqrt{g \cdot H}} = f_1\left(Re, Bn\right) \qquad (4)$$

$$\frac{S}{V^{1/3}} = f_2\left(Re, Bn\right) \qquad (5)$$

where Re and Bn are respectively the Reynolds and Bingham numbers, which are defined as follows:

$$Re = \frac{\rho \cdot V^{1/3} \cdot \sqrt{g \cdot H}}{\mu} \qquad (6)$$

and

$$Bn = \frac{\tau_o}{\rho \cdot g \cdot H} \qquad (7)$$

In this analysis, it is assumed that SCC matrix rheology can be adequately described by the Bingham model, with the yield stress, τ_O, and the plastic viscosity, μ, as the sole characteristic parameters. It can be argued that more sophisticated rheological models may be more accurate in describing the SCC rheology, in which case, the latter would be prescribed by more parameters than τ_O and μ in the dimensional analysis. However, in the scope of this paper, the study focuses in drawing primarily the connection between the intrinsic rheology of a mixture and its slump flow test measurement parameters.

3 EXPERIMENTAL METHODOLOGY

The role of rheology in the SCC matrix flow and its connection to the slump flow test parameters was examined by conducting a series of laboratory experiments in order to determine the generic effect of the dimensionless parameters. According to dimensional analysis, the slump flow test of any fluid of known rheology should produce similar dependence relations such as those in Equations 4 to 7. For example, to isolate the effect of viscosity on the flow, a series of tests with a Newtonian fluid of known viscosity, was conducted. A second series of experiments was conducted with Bingham fluids to address the effects of both viscosity and yield stress on flow. Once the generic relations between the dimensionless parameters were determined, a cement mortar (i.e. a mixture of cement, water and sand) was used in order to investigate whether these relations are valid for cement-based composites.

3.1 RHEOLOGICAL MEASUREMENTS

For both the Bingham and Newtonian fluids, a widely used commercially available rheometer was used for the measurement of the rheological parameters. Commercially available glycerine was used as the Newtonian fluid, and the variation of its viscosity was achieved by varying the temperature of the fluid in the range between 5 and 25°C; caution was taken in the process so that no temperature variations occurred within a single glycerine viscosity test in the rheometer. This was achieved by carrying out the test in a controlled environment and it was verified with temperature measurements of the sample before and after the measurement procedure. For the Bingham mixtures tests, a carbopol of acrylic acid cross-linked with a polyalkenyl polyether was used instead of SCC mixtures because the former is easy to produce while at the same time it is possible to alter and maintain its rheological parameters as well as reuse the mixture in repetitive tests. The rheological characteristics of the carbopol mixtures (viscosity and yield stress) were varied by altering the powder concentration during the preparation procedure of the mixture.

Viscosity measurements were conducted using cylindrical spindles and the viscosity value for each mixture was directly recorded from the digital reading of the rheometer. The yield stress measurements were conducted using vane spindles. For both types of measurement, the spindles used were according to the suggestions for optimum measurements from the manufacturer of the rheometer adopted in this study. The values of viscosity measured for glycerine, carbopol and cement mortar mixtures were obtained by direct measurement using Spindle No. 7 at a constant rotational speed set to 20 rpm in the rheometer set-up. The yield stress for Bingham fluids was also obtained by the same rheometer; these tests were carried out using Spindle V-73 at a rotational speed of 0.5 rpm. The measurements were tracked through a rheometer inbuilt software, providing in real time graphs of stress versus apparent strain and thereby deducing the yield stress value.

The rheological measurements using similar procedures were conducted for cement mortar samples with cement to sand ratio equal to 1/3. The sand used had a maximum aggregate size of 3 mm. The rheological characteristics of these samples were altered by varying the superplasticizer-to-cement ratio, which ranged between 0.076 and 0.087. These measurements were similarly obtained using the appropriate spindle at a rotational speed of 0.5 rpm, in the rheometer set-up. It should be noted that the tests were carried out on two different samples (Mortar 1 and Mortar 2). A typical output curve of the rheometer in order to determine the yield stress of the mixture is shown in Figure 2, The value of the yield stress is the stress value approached at near-zero apparent strain rate (towards the right-end of the curve). The measured rheological parameters (both viscosity and yield stress) of all the different fluid mixtures tested are provided in Table 1.

3.2 FLOW MEASUREMENT

The slump flow test was carried out using the unique experimental setup shown in Figure 3. The flow was captured with a high definition digital video camera. The video recording was done at a frame rate of 24 s^{-1}. The video capture was then analysed frame-by-frame using specialised video-image processing software in order to track the fluid flow front and thereby deduce the local flow velocity at various spread radii. It has to be noted that the flow velocity is measured in the horizontal direction.

4 RESULTS AND DISCUSSION

4.1 GENERAL SLUMP FLOW CHARACTERISTICS

In each series of experiments, the position of the moving front of the fluid flow was tracked and the front (spread) velocity was thereby deduced at each radial position. Figure 4a shows the variation of the spread velocity with the spread radius of the mixture, for a reference Newtonian fluid (glycerine at 10°C). In the flow process an accelerating regime is observed, in which the spread velocity is increasing up to a maximum due to a net driving force; this occurs up to a distance of 0.175 m (1.75 r_O). Thereafter a decelerating regime is observed, in which the spread velocity decreases (mainly due to the action of viscous forces) until the flow is brought to rest. This region extends up to a further distance of $2r_O$, reaching a final extent of up to 3.75 r_O. Similar qualitative flow characteristics were observed (Figure 4b) for the Bingham fluid (Carbopol); an accelerating and decelerating part are evident in the flow evolution, with the decelerating extent being much shorter than in the Newtonian case, due to the existence of a yield stress. For the Carbopol mixture with a concentration of 0.325 %w/w (Figure 4b), the final radial spread was measured at 0.31 m (3.1 r_O), while the extent of the corresponding decelerating region (up to the point where the flow is brought to rest) was measured as 0.08 m (0.8 r_O). It is worth noting that the trends described above were accurately reproduced for a number of experiments - even though the accuracy varied from mixture to mixture, depending on the speed of flow, which in turn affected the accuracy in the video frame capturing, and the sensitivity in the preparation of the mixture. Figure 5 shows the reproducible curves for two series of experiments, with glycerine and Carbopol.

The distinction between the various flow regimes is made through an examination of the flow velocity variation with the flow spread radius. Figure 6 shows this velocity variation over the spread radius for all the Carbopol mixtures investigated in this paper. The accelerating flow part for each of these mixtures has a different extent, and therefore this flow regime cannot be referenced at a constant spread radius; in other words, referencing the flow at a constant spread radius may represent different qualities of the flow. In particular, the extent of the accelerating regime (over which the only opposing dominant action is that of viscous forces) provides a measure of the viscosity of the flow; similarly, the extent of the decelerating regime is a measure of the yield stress. The classical application of the slump flow test as a SCC performance indicator, and the interpretation of the test in terms of fluid mechanics and rheology, raises two important issues: i) the reference spread of 500 mm for which practitioners report the time needed to be achieved, seems an arbitrary choice in terms of the fluid mechanical behavior, and ii) the measurement of the overall time for the flow to reach its final spread is an indicator of an integrated/averaged spread velocity, that could be somewhat loosely interpreted as bulk flow velocity.

4.2 THE EFFECT OF VISCOSITY ON THE SLUMP FLOW VELOCITY

The effect of viscosity can be derived by examining the local flow velocity of the Bingham fluid within the accelerating flow regime. However, as the identification of the extent of this regime in the Bingham fluid flow would pose further uncertainties into the analysis, the inertia regime has been experimentally modeled in the laboratory using a Newtonian fluid in a series of slump flow tests. In this way, it has been ensured that whatever the spread radius, the flow was measured and analysed without experiencing or being dominated by effects of yield stress - a characteristic that would be representing the decelerating/stagnating regime.

In the tests, the viscosity of the fluid was varied and the local flow velocity at different spread radii was measured. As per non-dimensional analysis (see Section 2), Figure 7 shows the variation of the non-dimensional velocity against the non-dimensional viscosity of the fluid, taken at 4 different radial spreads (300, 400, 500 and 600 mm). The results confirm that as the (non-dimensional) Newtonian viscosity of the fluid increases, the local flow velocity decreases, and this is valid for all referenced spread points. The effect of viscosity on the flow velocity becomes stronger and more evident as the flow evolves further away from the cone; this is verified by the steeper correlation slopes observed for the flow velocity at greater distances. The correlation between flow velocity and viscosity improves as the radial spread increases from 300 to 600 mm.

The experiments investigating the effect of viscosity were repeated with Carbopol mixtures, taking into account the fact that, yield stress dominates in a region near the final spread. Figure 8 shows the effect of viscosity on the measured local velocity for all Carbopol mixtures at the 300, 400, 500 and 600 mm radial spread positions. As expected, as the (non-dimensional) viscosity of the fluid increases, the local flow velocity decreases. Furthermore, the effect of viscosity on the flow velocity becomes stronger as the flow evolves further away from the initiation position; this is verified by the steeper correlation slopes observed for the flow velocity. If a better fit is sought for the non-dimensional reference velocity-viscosity relation, Figure 9 shows the in log-log plot of the local velocity at the 500mm-radial spread position versus the viscosity in both the Newtonian and Bigham cases.

4.3 THE EFFECT OF YIELD STRESS ON THE SLUMP FLOW VELOCITY

Figure 10 shows the effect of dimensionless yield stress on the dimensionless slump flow velocity in the Bingham fluid (Carbopol) tests, at the 4 reference radial spread positions mentioned before. Overall, it appears that the higher the yield stress of the fluid, the lower the local flow velocity at a given reference radial spread position. Specifically, in areas far away from the final spread (e.g. at the 300 mm for most tests) the flow velocity seems insensitive to the yield stress value while the strongest influence appears closer to the final spread of the flow (e.g. at 600 mm). This apparent effect of the yield stress on the flow velocity at increased radial spread position is rather superficial and the result of a spurious correlation. In terms of the fluid mechanics of the slump flow test, the action of yield stress is local and it is not apparent throughout the slump flow; the flow is retarding merely due to the viscous forces. Of course, the higher the yield stress of the fluid (for the same viscosity), the shorter the spread will be at which inertia stresses will match the yield stress, thereby reaching the flow stagnation point and final spread. In this series of experiments it was not possible to keep the viscosity of Carbopol mixtures constant while altering the yield stress value of the fluid mixture.

4.4 THE EFFECTS OF YIELD STRESS AND VISCOSITY ON THE FINAL SPREAD AND STOPPING TIME

The relation between the final spread and the rheology of the Bingham fluid was examined in two steps: (i) the effect of the yield stress and the viscosity of the fluid on the final spread was examined by using a range of Carbopol mixtures, and (ii) the applicability of the generic results drawn from the Carbopol mixtures was tested using a range of cement mortar samples, rheologically modeled as Bingham fluids. The results in Figure 11 show clearly that the dimensionless final spread is linearly related to the yield stress of the fluid mixture. The good correlation depicted denotes that the yield stress is indeed the dominant parameter affecting the final spread. The strong linear relation between the yield stress and the final spread is also confirmed when the cement mortar samples are tested. In fact, the three lines for the various sample tests have nearly the same slope and are only shifted by some distance across each other. This difference can be attributed to the different range of viscosities that the mixtures have, as shown in Figure 12, fitted by a curvilinearly decaying curve. For example, Carbopol mixtures exhibit much higher viscosities, which lead to lower final spreads (for equal yield stress). It has to be mentioned that similar observations to Figs. 11 and 12 can be found in the literature [21 - 27]. What is of particular interest is the observation that the slopes are approximately the same, given the uncertainties inherent in the experimental procedures. Hence, Equation 5 can be expressed from dimensional analysis as follows:

$$\frac{S}{V^{1/3}} = -A \cdot Bn + B \tag{8}$$

Equation 8 can be rearranged as follows:

$$\tau_o = \frac{\rho}{A'}(B' - S) \tag{9}$$

where only material constants are included. It should be noted that Equation 9 holds only for a certain range of *S* values. A three-parameter expression would be:

$$\tau_o = \frac{\rho}{A'}(B' - S) + C \tag{10}$$

The above model is of the same functional form as other expressions relating concrete yield stress to slump [7]. From these results, it appears that for cement mortars $A \approx$ -50 and $B \approx 5.5$. A further series of tests with cement mortars and other concrete mixtures can be used to assess the variability of these results and their accuracy.

Although it is clear that there is a linear relation between the final spread and the yield stress, there is a non-linear relation between the final spread and the plastic viscosity. The two sets (carbopol and cement mortar) seem to be similar and exponentially decaying with increasing non-dimensional viscosities (Figure 12). It has to be noted that there is a limited range in plastic viscosity values for cement mortars to extend this observation. Similarly, the final stopping time was also measured; this was obtained from the video sequence recorded for the mixture flow front and it was defined as the time elapsed for the moving front to stay stationary in two consecutive frames. The non-dimensional stopping time seems to decrease exponentially with non-dimensional plastic viscosity; in fact, for a value higher than 0.06 for the dimensionless viscosity, the dimensionless final spread remains almost constant. This can be attributed to the fact that above a critical value of plastic viscosity (and yield stress) the material tends not to spread but instead to produce a slump. Also, there seems to exist a similar exponentially decreasing relation between the final stopping time and the viscosity of the mixture. Figure 13 shows the variation between the viscosity and the final stopping time in the corresponding slump tests in dimensional and non-dimensional forms respectively. The figure shows that the higher the viscosity is, the shorter the final stopping time is. Although a mixture with higher viscosity would be linked to slower flow velocities, it is also true that such mixture will exhibit shorter final spread.

5 *CONCLUDING REMARKS*

Systematic measurements from an empirical characterisation test were performed, analysed and interpreted from a fluid mechanical approach in order to reveal the role of rheology and its connection to the empirical measurements of the slump test. Non-dimensional analysis reveals that there exist viscous and yield-stress dominated regions in the slump test flow, which need to be taken into consideration when empirical measurements are interpreted. Measurements which are representative of the viscosity would be indicative of the flowability of the tested mixture, while measurements which are representative of the yield stress of the tested fluid would be indicative of the onset of segregation. Our findings can be summarised as follows:

1. The time for a spread of 500 mm which is used as reference for measurement parameters, is rather an arbitrary choice; this is because the slump flow is experiencing both viscous and yield-stress effects in the flow extent of this spread, and thereby measurements may be representing different rheological characteristics (either viscosity or yield stress values of the tested fluid).
2. The final spread measurement is directly linked to the yield-stress of the tested fluid; the non-dimensional spread is linearly related to the non-dimensional yield stress of the fluid with a very good agreement for both the Carbopol and cement mortar mixtures. Moreover, the correlation lines appear to be parallel implying that this relation is universal. The observed shift is primarily due to the different viscosity value.
3. There are strong indications that the non-dimensional viscosity of the mixture is associated with the non-dimensional final spread as well as the non-dimensional stopping time of the slump flow. This set of experimental data suggests an exponential decay of the final spread and stopping time with viscosity; the precise relations remain to be confirmed with further experiments and simulations, which are beyond the scope of this manuscript.

ACKNOWLEDGEMENT

This work was supported by the University of Cyprus Internal Grant for Large Scale Multi-Disciplinary projects.

REFERENCES

[1] Roussel N: Correlation between yield stress and slump: Comparison between numerical simulations and concrete rheometer results, Mater Struct. 37 (2006) 469-477.
[2] Yahia A, Khayat KH: Applicability of rheological models to high-performance grouts containing supplementary cementitious materials and viscosity enhancing admixture, Mater Struct. 36 (2003) 402-412.
[3] Wallevik JE: Rheological properties of cement paste: Thixotropic behavior and structural breakdown, Cem. Concr. Res. 39 (2009) 14-29.
[4] Feys D, Verhoeven R, De Schutter G: Why is fresh self-compacting concrete shear thickening?, Cem. Concr. Res. 39 (2009) 510-523.
[5] Kou SC, Poon CS: Properties of self-compacting concrete prepared with recycled glass aggregate, Cem. Concr. Comp. 31 (2009) 107-113.
[6] Petrou MF, Wan B, Gadala-Maria F, Kolli VG, Harries KA: Influence of mortar rheology on aggregate settlement, ACI Mater. J. 97 (2000) 353-363.

To appear as: **Appl. Rheol. 20 (2010) 62402**
DOI: **10.3933/ApplRheol-20-62402**

[7] de Castro AL, Liborio JBL: Initial rheological description of high performance concretes, Mater. Res. 9 (2006) 405-410.
[8] Nielsson I, Wallevik O: Rheological evaluation of some empirical test methods – preliminary results, Proceedings of the 3rd International RILEM Symposium on Self Compacting Concrete, Reykjavik, Iceland (2003) 59-68.
[9] Feys D, Verhoeven R, De Schutter G: Evaluation of time independent rheological models applicable to fresh self-compacting concrete, Appl. Rheol. 17 (2007) 56244.
[10] Feys D, Verhoeven R, De Schutter G: Extension of the Poiseuille formula for shear thickening materials and application for self compacting concrete, Appl Rheol. 18 (2008) 62705.
[11] Ferraris CF: Testing and modeling of fresh concrete rheology, NISTIR 6094, National Institute of Standards and Technology, USA (1998).
[12] Larrard F de, Ferraris CF, Sedran T: Fresh concrete: A Herschel-Bulkley material, Mater. Struct. 31 (1998) 494-498.
[13] Wu Z, Zhang Y, Zheng J, Ding Y: An experimental study on the workability of self-compacting lightweight concrete, Constr. Build Mat. 23 (2009) 2087-2092.
[14] Chidiac S.E, Mahmoodzadeh F: Plastic viscosity of fresh concrete - A critical review of predictions methods, Cem. Concr. Res, doi: 10.1016/j.cemconcomp.2009.02.004.
[15] Okamura H: Self-Compacting High Performance Concrete, Concr. Int. Vol. 19 (1997) 50-54.
[16] Saak AW, Jennings HM, Shah SP: A generalized approach for the determination of yield stress by slump and slump flow, Cem. Concr. Res. 34 (2004) 363-371.
[17] Phan TH: Chaouche M: Rheology and stability of self-compacting concrete cement pastes, Appl. Rheol. 15 (2005) 336-343.
[18] Sun Z, Gregori A, Ferron R, Shah SP: Developing falling-ball viscometer for highly flowable cement-based materials, ACI Mater. J. 104 (2007) 180-186.
[19] Ferraris CF, Brower LE: Comparison of concrete rheometers, Concr. Int. 25 (2003) 41-47.
[20] Feys D, Verhoeven R, De Schutter G: Why is fresh self-compacting concrete shear thickening? Cem. Con. Res. 39 (2009) 510-523.
[21] Esping O: Slump flow values versus Bingham parameters for high flowable mortars and concretes, Proceedings of the 5th International RILEM Symposium – SCC 2007, Ghent, Belgium (2007) 315-322.
[22] Schowalter WR, Christensen G: Toward a rationalization of the slump test for fresh concrete: Comparisons of calculations and experiments, J. Rheol. 42 (1998) 865-870.
[23] Pashias N, Boger DV, Summers J, Glenister DJ: A fifty-cent rheometer for yield stress measurement, J. Rheol. 40 (1996) 1179-1189.
[24] Saak AW, Jennings HM, Shah SP: A generalized approach for the determination of yield stress by slump and slump flow, Cem. Concr. Res. 34 (2004) 363-371.
[25] Bartos PJM, Sonebi M, Tamimi AK: Workability and rheology of fresh concrete: Compendium of tests, RILEM, Cachan, France (2002).
[26] Koehler EP, Fowler DW: A portable rheometer for self-consolidating concrete, International Center for Aggregates Research, The University of Texas at Austin (2009).
[27] Esping O: Early age properties of self-compacting concrete, Ph.D. Thesis, Chalmers University of Technology, Göteborg, Sweden (2007).
[28] Roussel N, Coussot P: Fifty-cent rheometer for yield stress measurements: from slump to spreading flow, J. Rheol. 49 (2005) 705-718.
[29] Roussel N: A thixotropy model for fresh fluid concretes: theory, validation and applications, Cem. Concr. Res. 36 (2006) 1797-1806.
[30] Roussel N: A thixotropy model for fresh fluid concretes: Theory and applications, Proceedings of the 5th International RILEM Symposium – SCC 2007. 1, pp 267-272, Ghent, Belgium, Sept 3-5, 2007.
[31] Jarny S, Roussel N, Le Roy R, Coussot P: Thixotropic behavior of fresh cement pastes from inclined plane flow measurements, Appl. Rheol. 18 (2008) 14251.
[32] Wallevik JE: Relationship between the Bingham parameters and slump, Cem. Concr. Res. 36 (2006) 1214-1221.
[33] Petit JY, Wirquin E, Vanhove Y, Khayat K: Yield stress and viscosity equations for mortars and self-consolidating concrete, Cem. Concr. Res. 37 (2007) 655-670.
[34] Tregger N, Ferrara L, Shah SP: Identifying viscosity of cement paste from mini-slump-flow test, ACI Mater. J. 105 (2008) 558-566.
[35] Roshavelov TT: New viscometer for measuring flow properties of fluid concrete, ACI Mater. J. Vol. 102, pp. 397-404, 2005.
[36] Roussel N: Correlation between yield stress and slump: Comparison between numerical simulations and concrete rheometers results, Mater. Struct. 39 (2006) 501-509.
[37] Roussel N: The LCPC BOX: A cheap and simple technique for yield stress measurements of SCC, Mater. Struct. 40 (2007) 889-896.
[38] Tregger N, Ferrara L, Shah SP: Empirical relationships between viscosity and flow time measurements from mini-slump tests for cement pastes formulated from SCC, Proceedings of the 5th International RILEM Symposium – SCC 2007, Ghent, Belgium (2007) 273-278.
[39] Hu C: Rhéologie des bétons fluides, Etudes des Recherches des Laboratoires des Ponts et Chaussées, Paris, France (1995).
[40] Clayton S, Grice TG, Boger DV: Analysis of the slump test for on-site yield stress measurement of mineral suspensions, Int. J. Miner. Process. 70 (2003) 3-21.
[41] Roussel N, Stefani C, le Roy R: From mini cone test to Abrams cone test: measurement of cement based materials yield stress using slump tests, Cem. Concr. Res. 35 (2005) 817-822.
[42] Nguyen TLH, Roussel N, Coussot P: Correlation between L-box test and rheological parameters of a homogeneous yield

stress fluid, Cem. Concr. Res. 36 (2006) 1789-1796.
[43] Kurokawa Y, Tanigawa Y, Mori H, Nishinosono Y: Analytical study on effect of volume fraction of coarse aggregate on Bingham's constants of fresh concrete, Trans. Japan Concr. Inst. 18 (1996) 37-44.
[44] Thrane LN, Szabo P, Geiker M, Glavind M, Stang H: Simulation and verification of flow in SCC test methods, Proceedings of the 4th International RILEM Symposium on SCC, Chicago, USA (2005).
[45] Dufour F, Pijaudire-Cabot G: Numerical modeling of concrete flow: Homogeneous approach, Int. J. Numer. Anal. Methods Geomech. 29 (2005) 395-416.

FIGURE CAPTIONS

Table 1:Summary of experimental tests involving glycerine, Carbopol, and cement mortars.

Figure 1: A conceptual model for the evolving flow during the slump flow test.

Figure 2: Measurements depicting the yield stress; the above curve depicts the yield stress value of 53.5 Pa obtained for the Mortar 1 mixture with $8.3 \cdot 10^{-2}$ superplasticiser-to-cement ratio (listed in Table 1) using Vane Spindle V-73 at a rotational speed 0.5 rpm.

Figure 3: (a) Experimental arrangement, (b) resulting flow and (c) image analysis for a typical Carbopol test.

Figure 4: Spread velocity versus spread radius for (a) glycerine mixture at 10°C and (b) Carbopol at 0.325 %w/w concentration.

Figure 5: Spread velocity versus spread radius for repeated experiments on (a) glycerine at 10°C and (b) Carbopol of concentration 0.325 %w/w.

Figure 6: Variation of the spread velocity with radius of spread for the different Carbopol mixtures.

Figure 7: Variation of the dimensionless local flow velocity with dimensionless viscosity for a Newtonian fluid (glycerine) for (a) 300 mm, (b) 400 mm, (c) 500 mm, and (d) 600 mm radial spreads.

Figure 8: Variation of the dimensionless local flow velocity with dimensionless plastic viscosity for a Bingham fluid (Carbopol) for (a) 300 mm, (b) 400 mm, (c) 500 mm, and (d) 600 mm radial spreads.

Figure 9: The log-log variation of non-dimensional velocity at reference radial spread of 500mm for the Newtonian (glycerine) and Bingham (Carbopol) fluid flow.

Figure 10: Variation of dimensionless velocity at (a) 300 mm, (b) 400 mm, (c) 500 mm, and (d) 600 mm with dimensionless yield stress for all the Carbopol mixtures.

Figure 11: Dimensionless final spread versus dimensionless yield stress for Carbopol and cement mortars.

Figure 12: Dimensionless final spread versus dimensionless plastic viscosity for Carbopol and cement mortars.

Figure 13: The dimensional (a) and non-dimensional (b) variation of the final spread versus plastic viscosity for Carbopol and cement mortars.

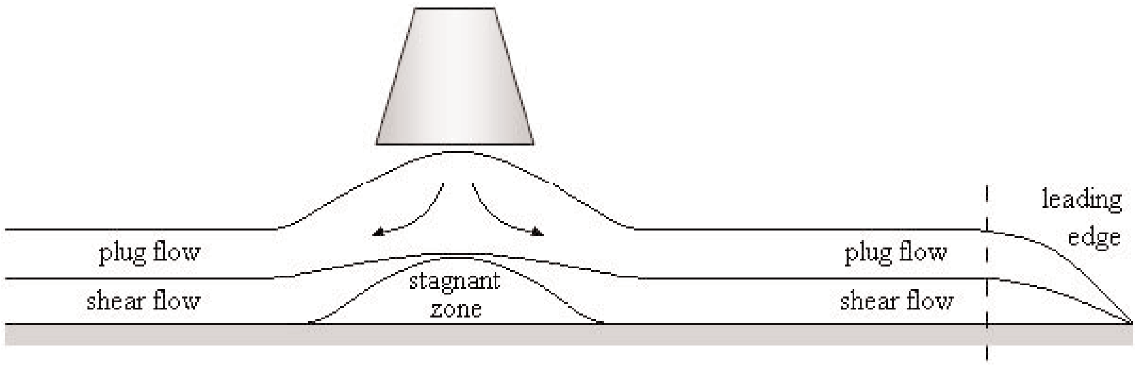
leading
edge
plug flow
shear flow
stagnant
zone
plug flow
shear flow

1

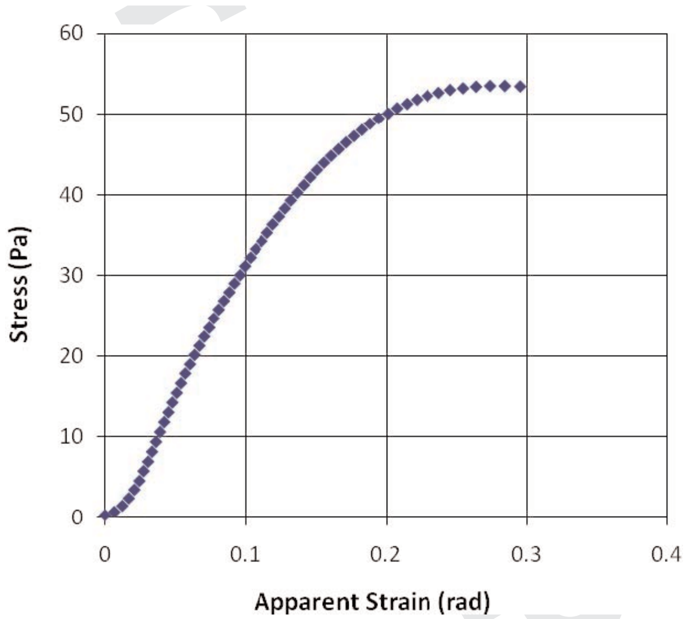
60
50
40
30
20
10
0
Stress (Pa)
0
0.1
0.2
0.3
0.4
Apparent Strain (rad)

2

3a

Applied Rheology
To appear as: Appl. Rheol. 20 (2010) 62402
DOI: 10.3933/ApplRheol-20-62402

3b

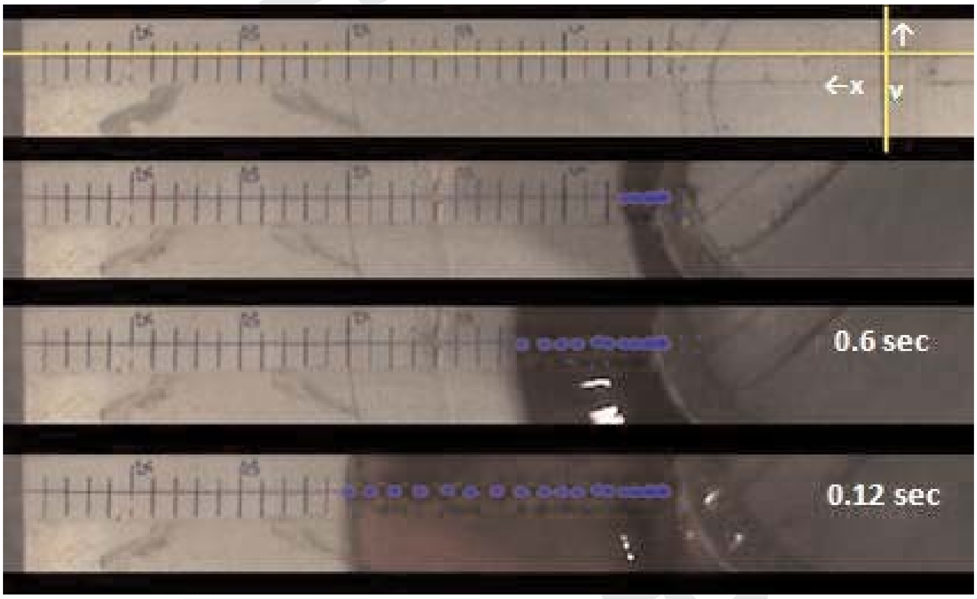

3c

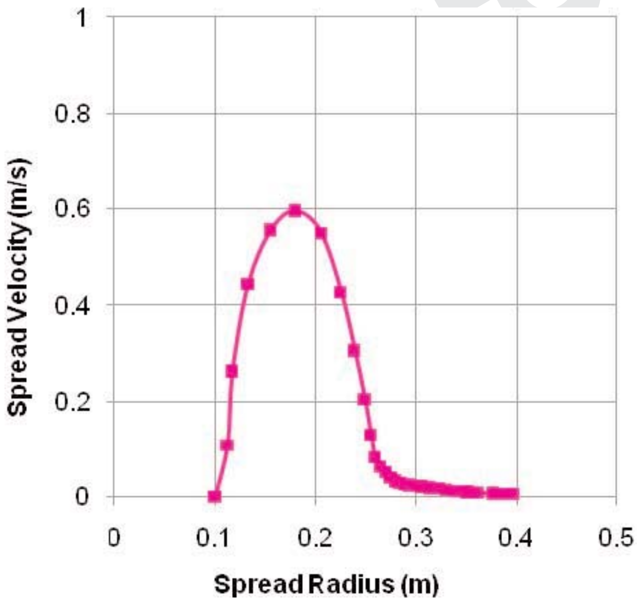

4a

To appear as: Appl. Rheol. 20 (2010) 62402
DOI: 10.3933/ApplRheol-20-62402

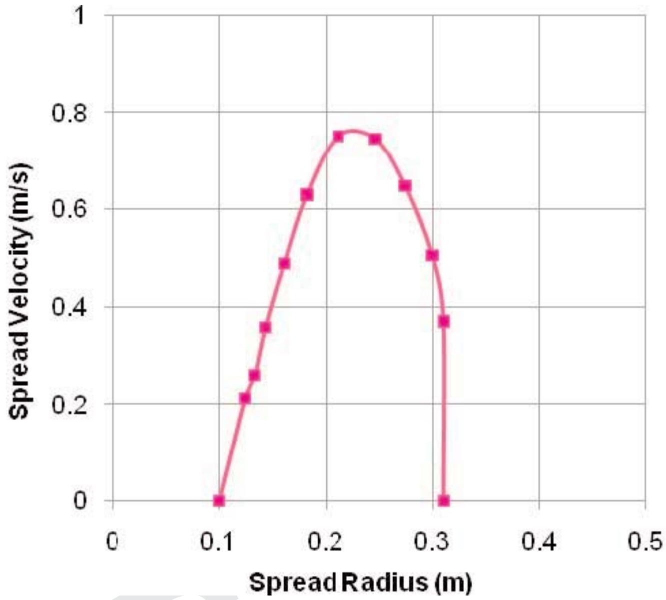

4b

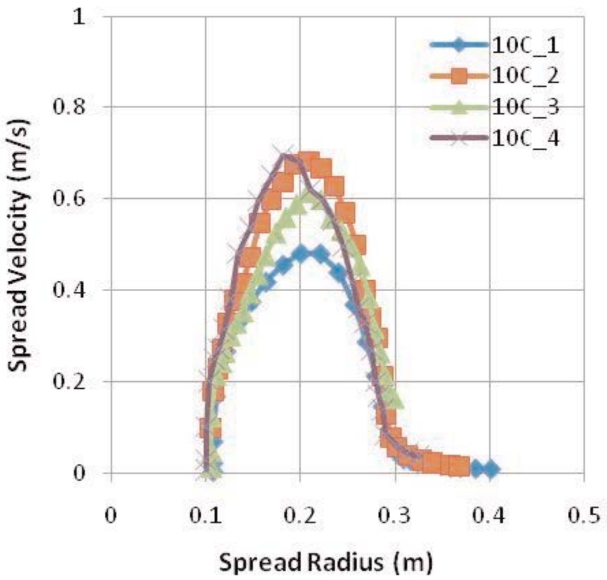

5a

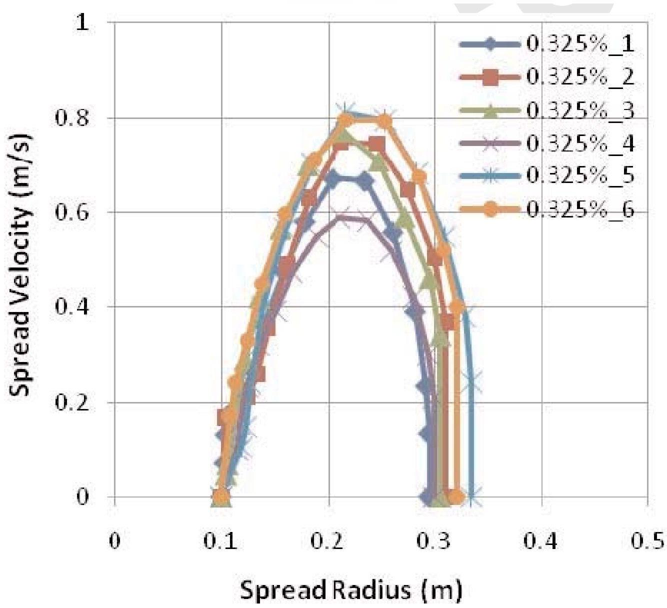

5b

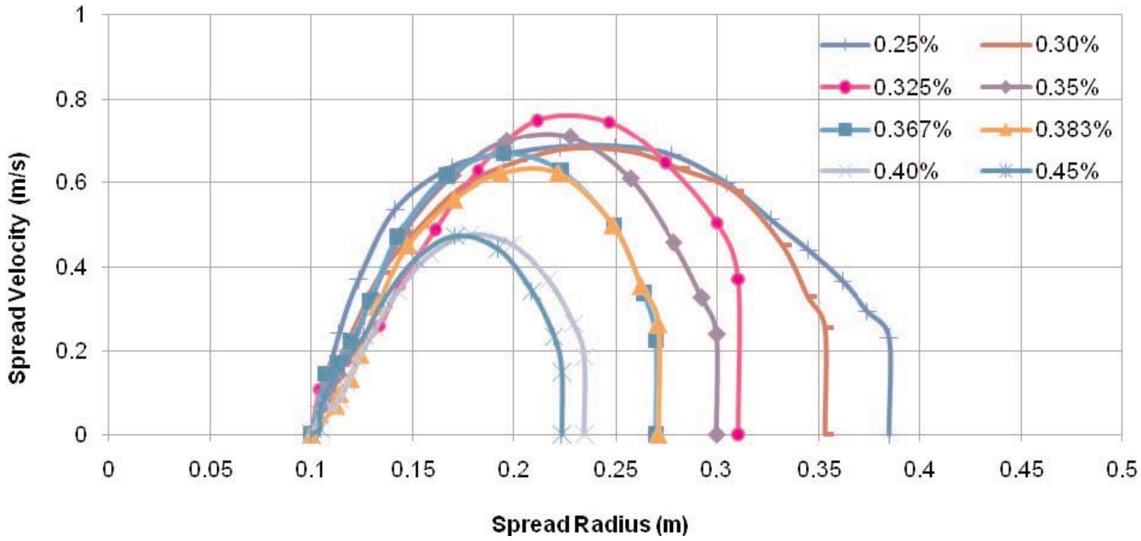
0.25%
0.30%
0.325%
0.35%
0.367%
0.383%
0.40%
0.45%
Spread Velocity (m/s)
Spread Radius (m)
1
0.8
0.6
0.4
0.2
0
0
0.05
0.1
0.15
0.2
0.25
0.3
0.35
0.4
0.45
0.5

6

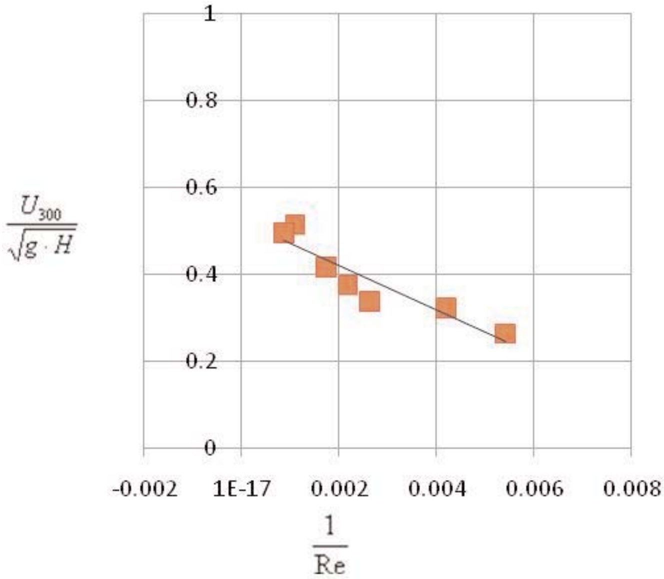
$\frac{U_{300}}{\sqrt{g \cdot H}}$
$\frac{1}{\mathrm{Re}}$
1
0.8
0.6
0.4
0.2
0
-0.002
1E-17
0.002
0.004
0.006
0.008

7a

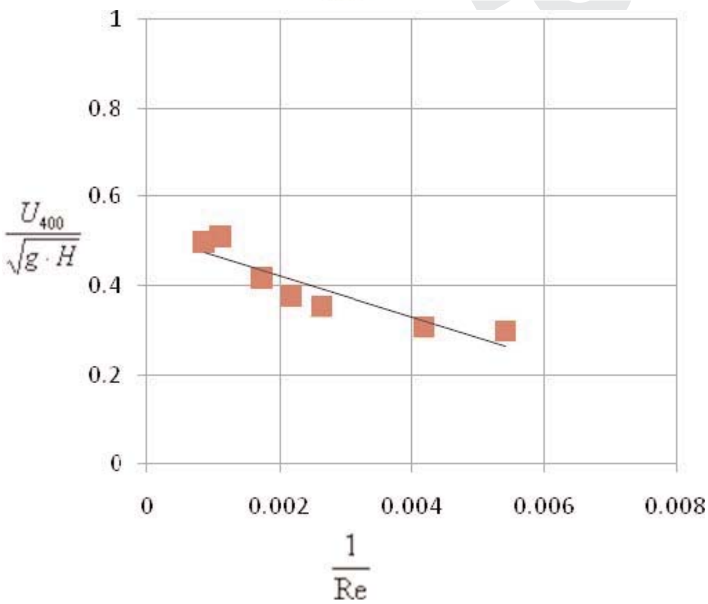
$\frac{U_{400}}{\sqrt{g \cdot H}}$
$\frac{1}{\mathrm{Re}}$
1
0.8
0.6
0.4
0.2
0
0
0.002
0.004
0.006
0.008

7b

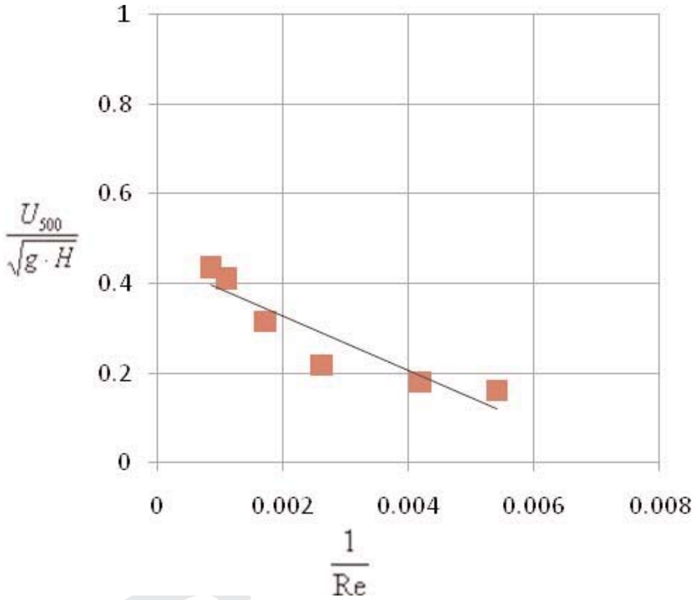
1
0.8
0.6
0.4
0.2
0
$\frac{U_{500}}{\sqrt{g \cdot H}}$
0
0.002
0.004
0.006
0.008
$\frac{1}{\mathrm{Re}}$

7c

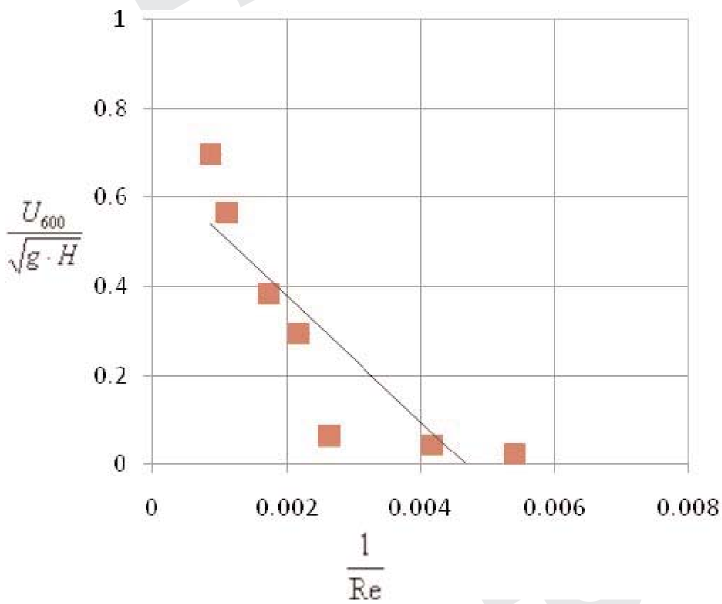
1
0.8
0.6
0.4
0.2
0
$\frac{U_{600}}{\sqrt{g \cdot H}}$
0
0.002
0.004
0.006
0.008
$\frac{1}{\mathrm{Re}}$

7d

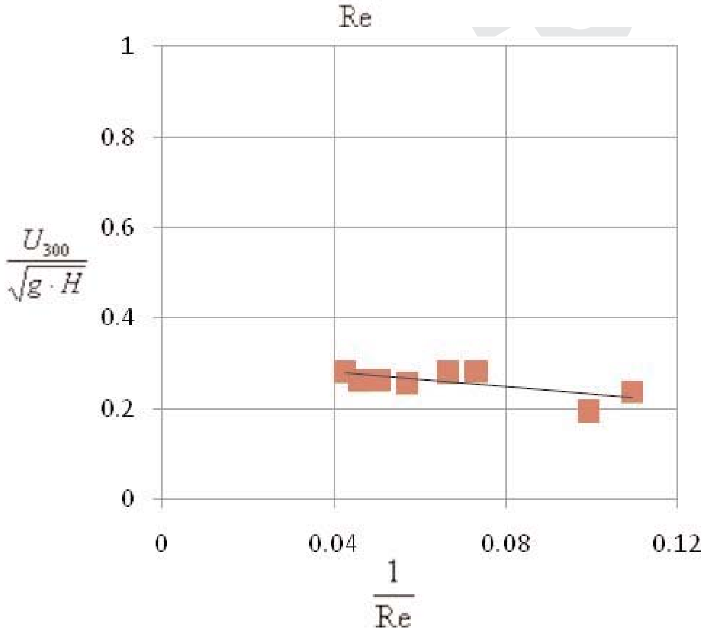
1
0.8
0.6
0.4
0.2
0
$\frac{U_{300}}{\sqrt{g \cdot H}}$
0
0.04
0.08
0.12
$\frac{1}{\mathrm{Re}}$

8a

To appear as: Appl. Rheol. 20 (2010) 62402
DOI: 10.3933/ApplRheol-20-62402

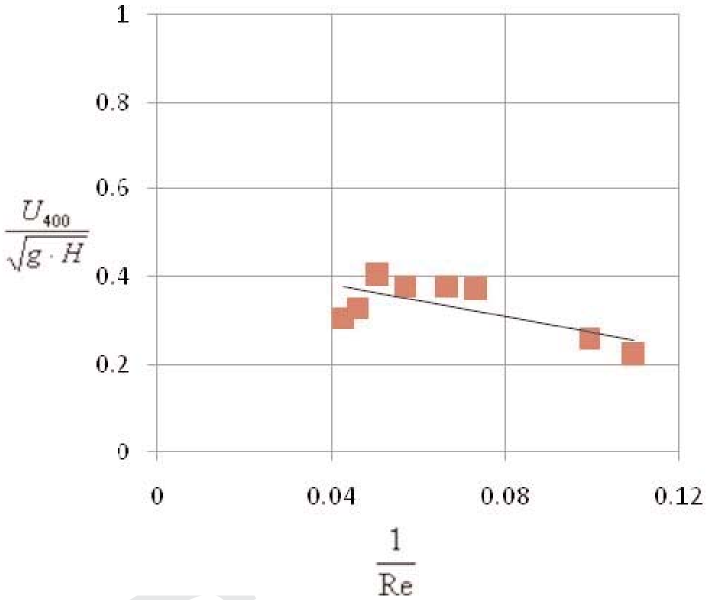

8b

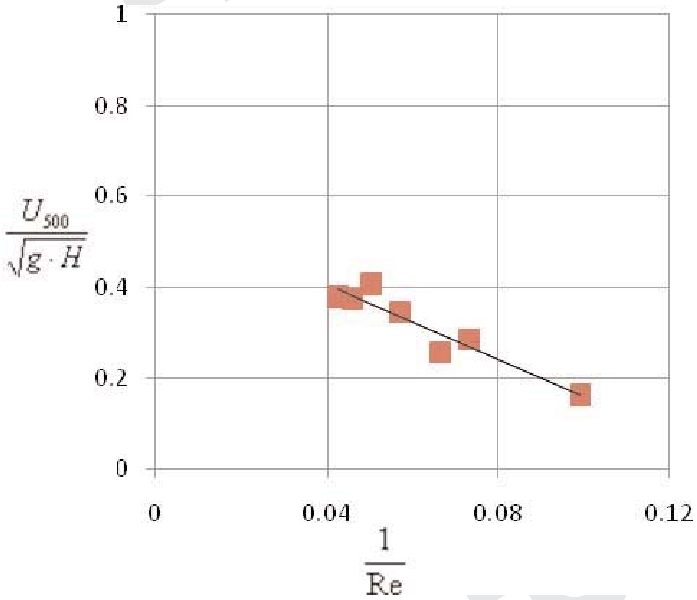

8c

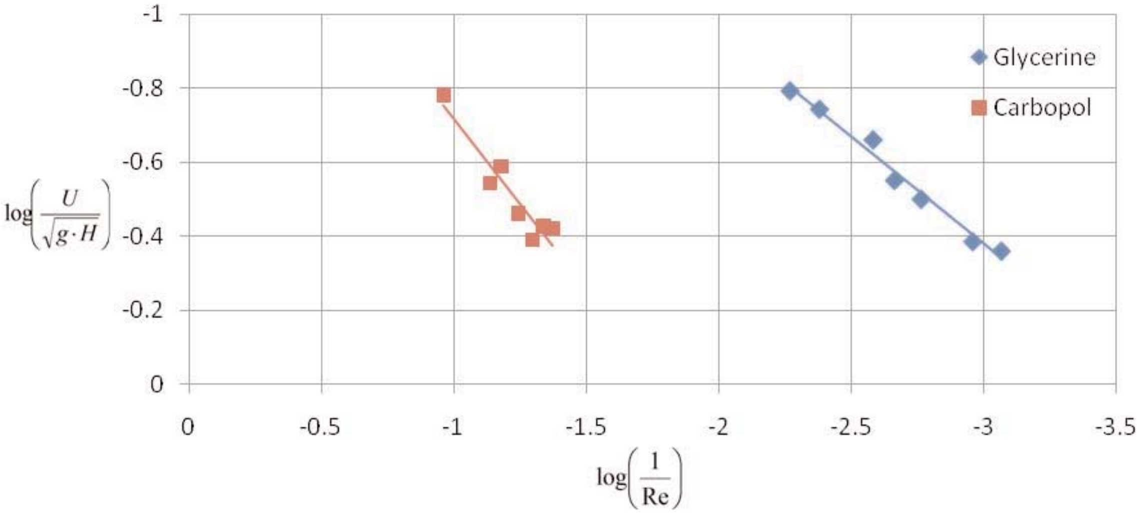

9

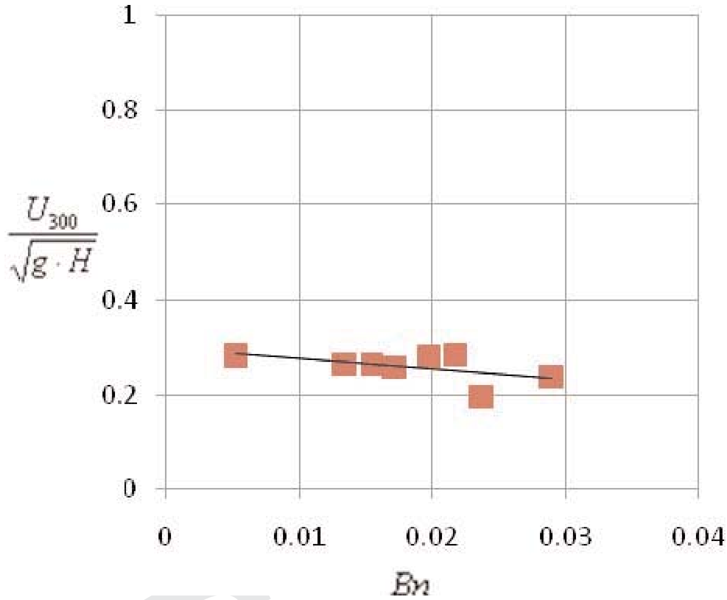
1
0.8
0.6
0.4
0.2
0
0
0.01
0.02
0.03
0.04
Bn

10a

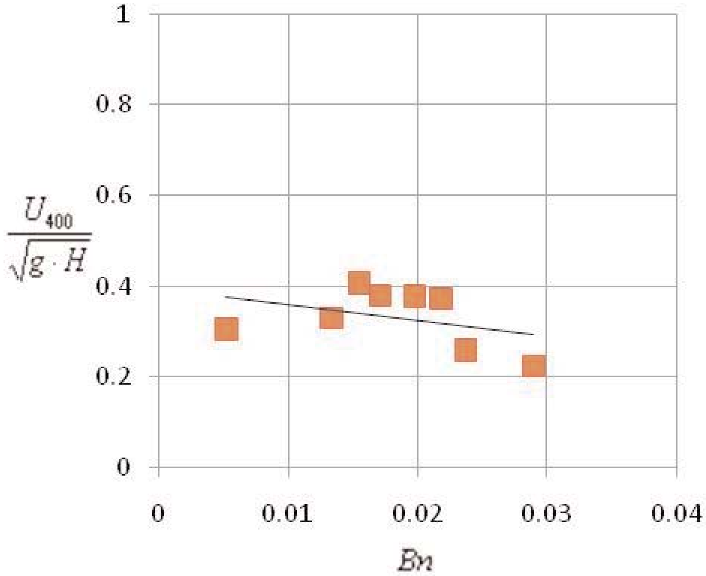
1
0.8
0.6
0.4
0.2
0
0
0.01
0.02
0.03
0.04
Bn

10b

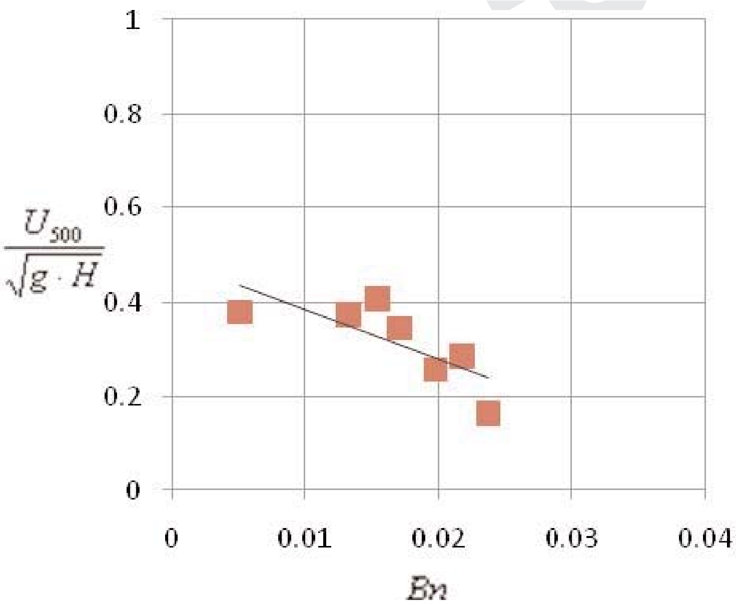
1
0.8
0.6
0.4
0.2
0
0
0.01
0.02
0.03
0.04
Bn

10c

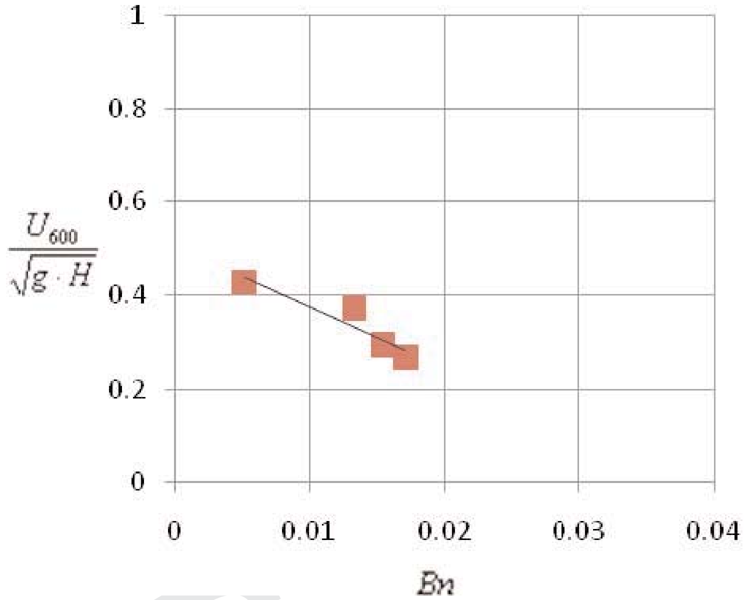
1
0.8
0.6
0.4
0.2
0
0
0.01
0.02
0.03
0.04
Bn

10d

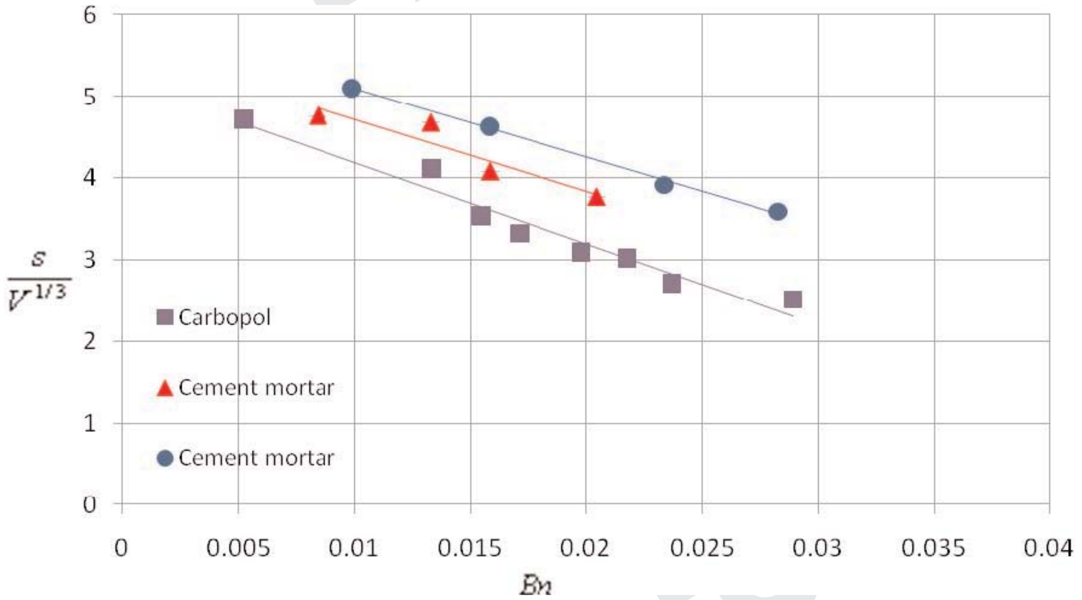
Carbopol
Cement mortar
Cement mortar
0
0.005
0.01
0.015
0.02
0.025
0.03
0.035
0.04
Bn

11

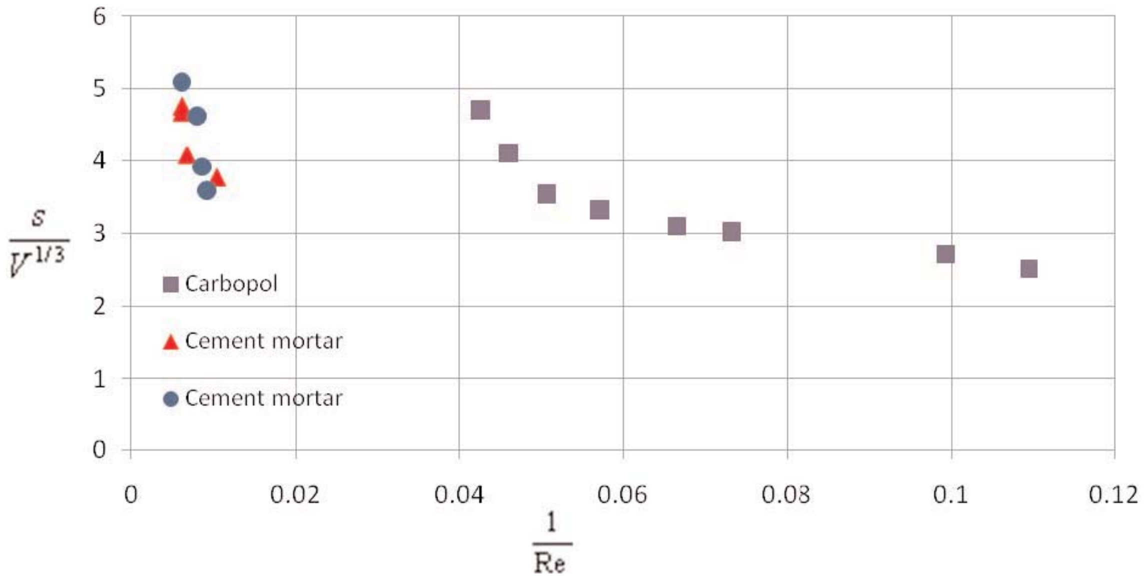
Carbopol
Cement mortar
Cement mortar
0
0.02
0.04
0.06
0.08
0.1
0.12

12

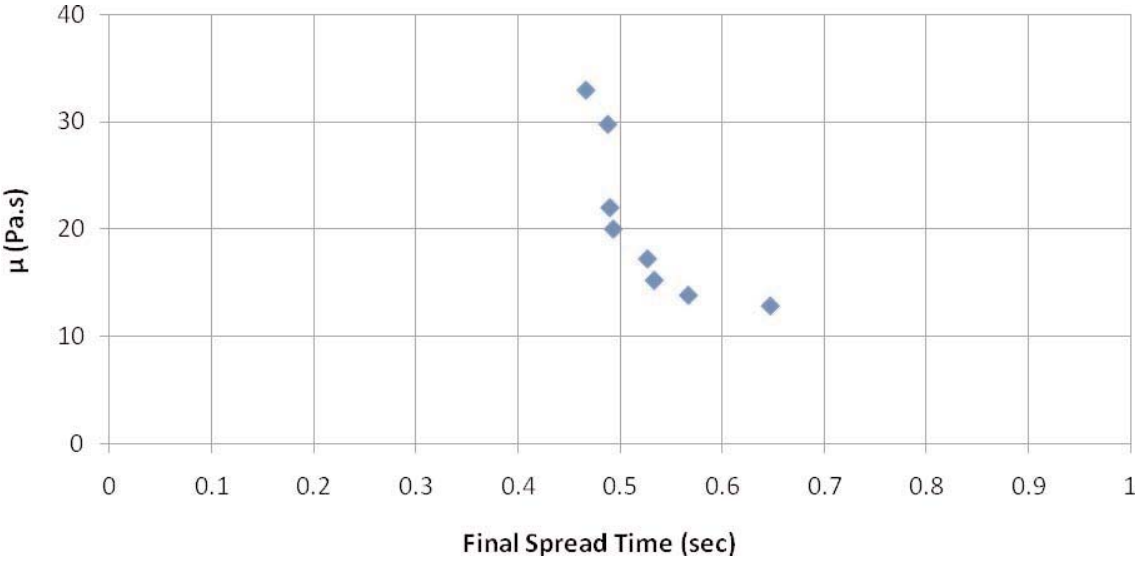

13a

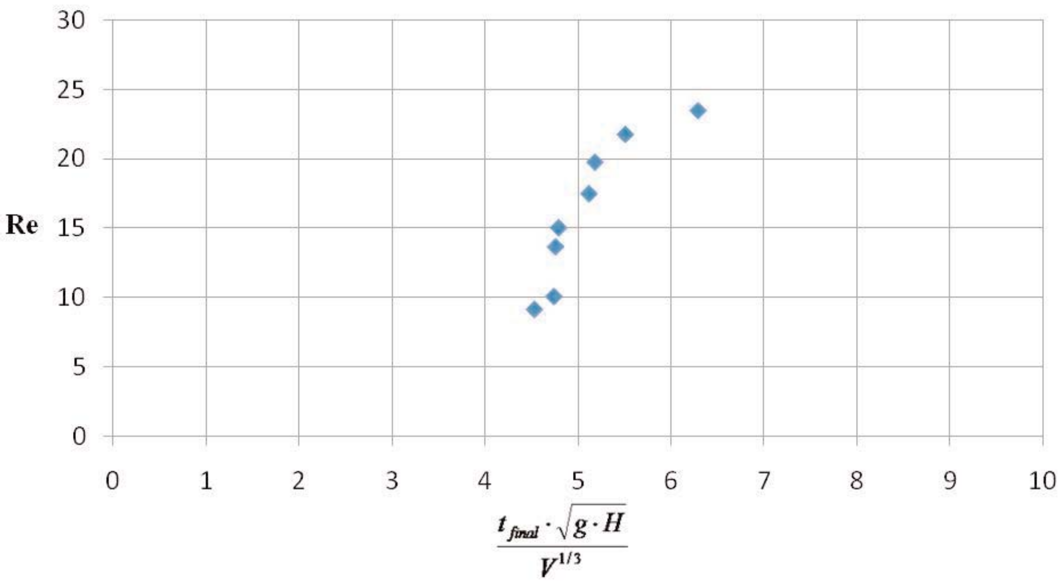

13b

<table>
<tr><th colspan="2">Glycerine</th><th colspan="3">Carbopol</th><th colspan="4">Cement Mortar</th></tr>
<tr><th>T (°C)</th><th>μ (Pas)</th><th>Concentration (% w/w)</th><th>μ (Pas)</th><th>τ_o (Pa)</th><th colspan="2">Superplasticizer / Cement (x10⁻²)</th><th>μ (Pas)</th><th>τ_o (Pa)</th></tr>
<tr><td>5</td><td>2.1</td><td>0.250</td><td>12.8</td><td>15.3</td><td rowspan="4">Mortar1</td><td>7.6</td><td>6.8</td><td>130.0</td></tr>
<tr><td>7</td><td>1.6</td><td>0.300</td><td>13.8</td><td>38.9</td><td>7.8</td><td>4.4</td><td>100.7</td></tr>
<tr><td>10</td><td>1.0</td><td>0.325</td><td>15.2</td><td>45.2</td><td>8.1</td><td>4.0</td><td>84.5</td></tr>
<tr><td>13</td><td>0.8</td><td>0.350</td><td>17.2</td><td>50.1</td><td>8.3</td><td>4.0</td><td>53.5</td></tr>
<tr><td>15</td><td>0.7</td><td>0.367</td><td>20.0</td><td>57.8</td><td rowspan="4">Mortar 2</td><td>7.9</td><td>6.0</td><td>179.9</td></tr>
<tr><td>20</td><td>0.4</td><td>0.383</td><td>22.0</td><td>63.6</td><td>8.2</td><td>5.6</td><td>148.5</td></tr>
<tr><td>25</td><td>0.3</td><td>0.400</td><td>29.8</td><td>69.1</td><td>8.4</td><td>5.2</td><td>100.5</td></tr>
<tr><td>-</td><td>-</td><td>0.450</td><td>33.0</td><td>84.8</td><td>8.7</td><td>4.0</td><td>62.8</td></tr>
</table>

1